Climate Data Record (CDR) Program

Climate Algorithm Theoretical Basis Document (C-ATBD)

NOAA MSU/AMSU-A Mean Layer Temperature

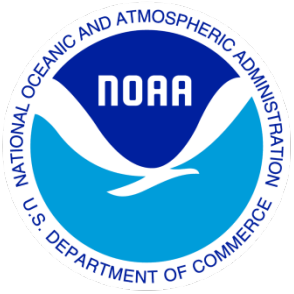

CDR Program Document Number: CDRP-ATBD-0682
Configuration Item Number: 01B-25
Revision 1 / April 6, 2015

REVISION HISTORY

Rev.	Author	DSR No.	Description	Date
1	Cheng-Zhi Zou and Jian Li NOAA/NESDIS/STAR	DSR-860	Initial Submission to CDR Program	04/06/2015

TABLE of CONTENTS

LIST of FIGURES

LIST of TABLES

1. Introduction

1.1 Purpose

The purpose of this document is to describe the algorithm submitted to the National Climatic Data Center (NCDC) by Cheng-Zhi Zou at NOAA/NESDIS/Center for Satellite Applications and Research that will be used to create the NOAA MSU/AMSU-A Mean Layer Temperature Climate Data Record (CDR), using the Microwave Sounding Unit (MSU) and Advanced Microwave Sounding Unit-A (AMSU-A) onboard historical NOAA polar orbiting satellites TIROS-N through NOAA-18, and EUMETSAT MetOp-A as well as NASA Aqua. The actual algorithm is defined by the computer program (code) that accompanies this document, and thus the intent here is to provide a guide to understanding that algorithm, from both a scientific perspective and in order to assist a software engineer or end-user performing an evaluation of the code.

1.2 Definitions

The following is a summary of the phrases and symbols used to define the algorithm.

Atmospheric Layer Temperature (or Mean Layer Temperature or Deep-Layer Atmospheric Temperature): Averaged brightness temperatures of those binned into grid cells within a predefined time interval. Since MSU brightness temperature comes from a weighted average of temperatures in a layer of the atmosphere with different levels within the layer having different weightings to the average, the gridded brightness temperature is thus interpreted as atmospheric layer temperature or mean layer temperature

Brightness Temperature: Satellite observation at the top of the atmosphere at each scan position; it is converted from *Radiance* using the Planck Function with instrument channel frequency as the input

Radiance: Satellite observation of the radiation emitted to space from the earth and atmosphere; it is converted from raw counts data of satellite observations using instrument calibration equation. Refer to 'CDRP C-ATBD: MSU/AMSU Radiance FCDR Derived from Integrated Microwave Inter-Calibration Approach' for derivation of radiances from satellite raw counts data

Diurnal Drift Correction: It adjusts the scene brightness temperatures at different observational times from all different satellites to the 12-noon local time using the following equation

$$T_{ba}(\mathbf{X}, t_{12-noon}) = T_{bu}(\mathbf{X}, t) - \Delta T$$

where

$T_{bu}(\mathbf{X},t)$ = IMICA-calibrated, limb-adjusted Level-1C scene brightness temperature at geo-location **X** and time *t*

$T_{ba}(\mathbf{X},t_{12-noon})$ = the adjusted brightness temperature at the 12-noon local time

$\Delta T = T_{bs}(\mathbf{X},t) - T_{bs}(\mathbf{X},t_{12-noon})$ = estimated diurnal anomaly from model simulations

Removal of Warm Target Effect: Removing warm target effect requires solving the following multi-satellite regression equations:

$$T_{ba} = T_{bu} + b_j - b_k + a_j T_w^{'}(j) - a_k T_w^{'}(k)$$

where

T_{ba} = adjusted brightness temperature after removing warm target effect

T_{bu} = IMICA-calibrated, limb-adjusted level-1c scene brightness temperature

$T_w^{'}$ = global ocean mean warm target temperature anomaly

j = satellite *index* running from all satellites involved in the calculation

k= satellite *index* running from all satellites involved in the calculation

b_j= constant regression coefficients to be solved

b_k= constant regression coefficients to be solved

a_j = warm target factor for satellite *j*, a regression coefficient to be solved

a_k=warm target factor for satellite *k*, a regression coefficient to be solved

Correction of Sensor Incidence Angle Effect (or Limb Correction): It adjusted brightness temperatures measured at off-nadir viewing angles to those close to nadir views. Statistical techniques and model simulations were both employed for limb-corrections in the MSU and AMSU-A observations. details are shown in relevant sections

Frequency Adjustment: MSU and AMSU-A were designed with different channel frequencies for their equivalent channels. Frequency adjustments derived from radiative transfer model simulations were applied on AMSU-A channels 5, 7, and 9 for each scan positions, which converted AMSU-A channels to MSU equivalent-channels 2, 3, and 4 for best merging accuracy

Three types of data sets are frequently discussed in this document. Unless otherwise specified, these data types are defined as follows:

Level-1C data: Orbital data containing IMICA calibrated swath radiances at scan positions as well as other satellite geo-location and calibration information taken from satellite Level-1b files

Level-3 data: Gridded dataset generated from Level-1C data for individual satellites; they are actually the atmospheric layer temperature for individual satellites

Merged Mean Layer Temperature Products: Merged Level-3 data products (layer temperature) from multiple satellites

1.3 Document Maintenance

MSU observation had stopped since 2007 and it was replaced by its successor, Advanced Microwave Sounding Unit-A (AMSU-A) since 1998. The polar orbiting satellites carrying AMSU-A instrument included NOAA-15, -16, -17, -18, -19, MetOp-A, MetOp-B, and EOS Aqua. Most of these satellites are still operating at the time of this writing and new observations are being added to the existing dataset every day. The merging algorithm for generating the atmospheric layer temperature Thematic Climate Data Record (TCDR) from MSU and AMSU-A observations was based on current understanding of the data issues and bias characteristics of the observations. New data issues and improved understanding of the old data issues may often occur when new observations become available. As such, algorithm updates and data version upgrade will be expected for the merged MSU and AMSU data products in the future which may result in improved understanding of the atmospheric temperature trends. If a change does occur, the document will be rewritten to incorporate algorithm updates and new findings.

2. Observing Systems Overview

2.1 Products Generated

Three channel-based, monthly gridded atmospheric layer temperature TCDR are generated by using merging algorithms described in this document and previous publications. These are temperatures of middle-troposphere (TMT), upper-troposphere (TUT), and lower-stratosphere (TLS), corresponding to measurements from MSU channels 2, 3, and 4 and their equivalent AMSU-A channels 5, 7, and 9, respectively. Table 2-1 lists the vertical coverage and spatial resolution of these products, which are derived from 16 polar orbiting satellites including TRIOS-N and NOAA-6 through NOAA-18, as well as EUMETSAT MetOp-A and NASA Aqua, covering time period from November 1978 through present.

Table 2-1 Products generated in this CDR, which are 36+ year-long, global monthly data with 2.5° latitudes by 2.5° longitudes grid resolution

Products	MSU/AMSU-A channels	Vertical Layer Coverage
TMT (Temperature Middle Troposphere)	2/5	Surface-15km
TUT or TTS (Temperature Upper Troposphere or Temperature Troposphere Stratosphere)	3/7	3-20 km
TLS (Temperature Lower Stratosphere)	4/9	12-26km

2.2 Instrument Characteristics

MSU and AMSU-A are both cross-track, line-scanned instruments designed to measure Earth radiation emitted by the atmospheric oxygen. The detailed system parameters and measurement principles for MSU and AMSU-A can be found in Kidwell (1998) and Robel et al. (2009). The following sections summarize only characteristics of the instruments related to the inter-calibration and TCDR development.

2.2.1 MSU

The MSU on board NOAA polar orbiting satellite series had been the primary instruments for measuring upper-air temperature profiles under all weather conditions, excluding precipitation, during 1978-2007. MSU was a microwave radiometer with four-channels to make passive measurements in the 5.5 millimeter oxygen region. The four channels responded to the following spectral frequencies: 50.3, 53.74, 54.96, and 57.95 GHz, respectively, with a channel bandwidth of 200 MHz in each case and a typical NEΔT (radiometric noise) of 0.3K. The radiance measured by each frequency channel comes

from a different layer of the atmosphere, depending on the strength of the absorption at that frequency. The percentage contribution of individual levels within the layer to the measured layer temperature is represented by a vertical weighting function, which is typically bell-shaped, peaking at a certain level in the height coordinate (Figure 2-1; the lower parts of the near surface channels are often cut off by the surface). Among these, MSU channel 1 (50.3 GHz) measured surface temperature, and channels 2, 3 and 4 measured temperatures of the middle-troposphere (TMT), upper-troposphere (TUT), and lower-stratosphere (TLS) with their weighting functions peaking respectively near 550, 250, and 100 hPa (Figure 2-1).

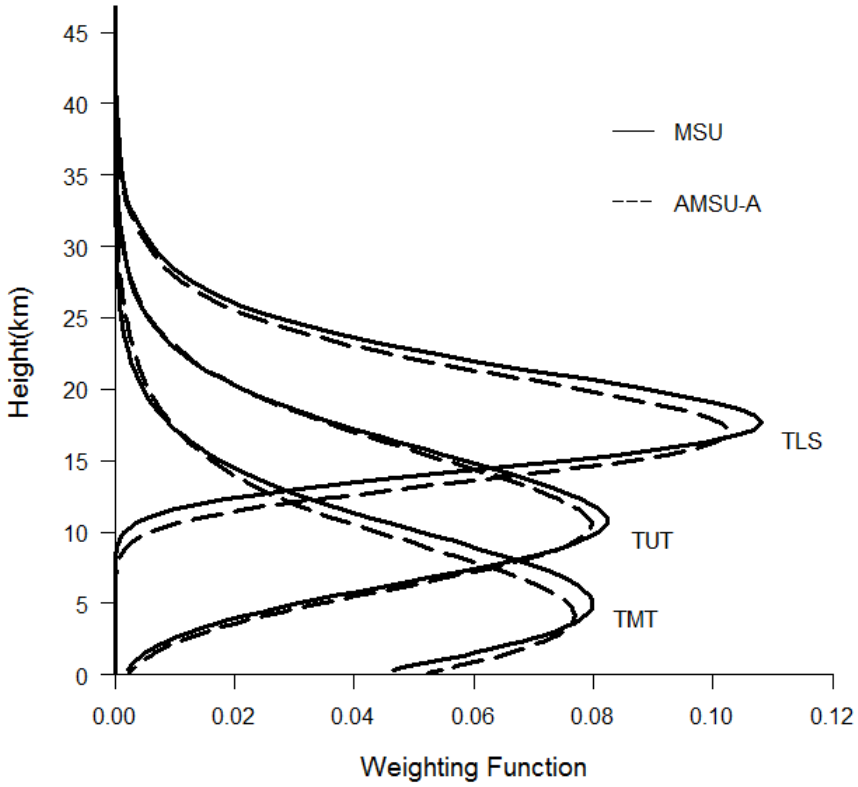

Figure 2-1 Weighting functions for the three MSU (solid lines) and AMSU-A (dashed lines) atmospheric channels that measure temperatures of the middle-troposphere (TMT), upper-troposphere (TUT), and lower-stratosphere (TLS). The weighting functions correspond to nadir observing conditions for the US standard atmospheric temperature profile.

The MSU was flown on nine sequential NOAA polar-orbiting satellites: TIROS-N and NOAA-6 through NOAA-14. The MSU was a cross-scanning instrument making eleven

Earth observations during each cross-track scan. The MSU sensors consisted of two four-inch diameter antennas named as MSU-1 and MSU-2. Each of the two antennas had an IFOV of 7.5 degrees. The MSU-1 was used by channels 1 and 2 while MSU-2 by channels 3 and 4. The antennas were step scanned through eleven individual 1.84-second Earth viewing steps and required a total of 25.6 seconds to complete (Kidwell, 1998). The MSU instrument parameters are summarized in Table 2-2.

Table 2-2 MSU instrument parameters

Cross-track scan angle (degree from nadir)	±47.35				
Scan time (second)	25.6				
Number of steps	11				
Angular FOV (degree)	7.5				
Step angle (degree)	9.47				
Step time (second)	1.84				
Ground IFOV at nadir (km diameter)	109.3				
Ground IFOV at end of scan	323.1 km cross-track 178.8 km along-track				
Distance between IFOV centers (km along-track)	168.1				
Swath width (km)	±1174				
Time between start of each scan line (second)	25.6				
Step and dwell time (second)	1.81				
Time difference between the start of each scan and the center of the first dwell period (second)	0.9				
Total channels	4				
Channel frequencies (GHz)	CHs	1	2	3	4
	Frequency	50.30	53.74	54.96	57.95
Instrument antenna systems	MSU-1 and MSU-2				
Responsible antennas for each channel	MSU-1 for channels 1 and 2 MSU-2 for channels 3 and 4				
Channel bandwidth (MHz)	200				
Black body and space view per scan line	1				
PRTs on each warm target	2				

2.2.2 AMSU-A

Since 1998, AMSU-A onboard NOAA-15 and its follow-on satellites has replaced MSU. As a successor to the MSU instrument, AMSU-A has improved instrument accuracy, and with its 15 channels provides finer vertical resolution and measurements well into the upper stratosphere. At each channel frequency, the AMSU-A antenna beam-width is a constant of 3.3 degrees. Thirty contiguous scene resolution cells are sampled in a stepped-scan fashion every eight seconds, each scan covering 48.33 degrees on each side of the nadir direction. These scan patterns and geometric resolution translate to a 45 km diameter cell at nadir and a 2,343 km swath width from the 833 km nominal orbital altitude. Among all discrete frequency channels, channels 5, 7, and 9 share a similar spectrum frequency with MSU channel 2, 3, and 4, respectively [Figure 2-1]. After conducting frequency adjustment on each individual channel, equivalent MSU channels can be obtained from the three AMSU-A channels to combine with MSU observations to produce merged mean layer temperatures.

Table 2-3 and Table 2-4 summarize the AMSU-A instrument parameters.

Table 2-3 AMSU-A instrument parameters

Cross-track scan angle (degree from nadir)	±48.33			
Scan time (second)	5.965			
Number of steps	30			
Step angle (degree)	3.33			
Step time (second)	0.1988			
Ground IFOV at nadir (km diameter)	50			
Swath width (km)	±1171			
Time between start of each scan line (second)	8			
Step and dwell time (second)	0.1988			
Total channels	15			
Channel Frequencies (GHz)	CHs:	5	7	9
	Frequency	53.60	54.94	57.29

Table 2-4 Channel and scanning view parameters for each AMSU-A antenna systems.

Instrument Antenna Systems	**A1-1**	**A1-2**	**A2**
Channel	6-7,9-15	3-5,8	1-2
Earth views per scan line	30	30	30
Blackbody and space view per scan line	2	2	2

PRTs in each warm target	5	5	7

3. Algorithm Description

3.1 Algorithm Overview

The main purpose of the merging algorithm is to derive homogeneous temperature CDR from the sequential overlapping MSU and AMSU-A observations onboard NOAA/EUMETSAT/NASA polar orbiting satellites channel by channel. Deriving such time series requires a number of steps:

- Inter-calibrating the satellite sensors
- Adjusting observations made at different viewing angles to nadir views (limb effect)
- Removing instrument temperature effects on observations
- Adjusting the observations to a common reference time (usually chosen as local noon time) to minimize diurnal effect related to satellite orbital drifts
- Adjusting AMSU-A temperatures due to their channel frequency differences from MSU
- Removing residual inter-satellite biases and their drifts

The Level-1c radiance data used for deriving the layer temperature TCDR were already inter-calibrated by the Integrated Microwave Inter-Calibration Approach (IMICA, formerly known as the simultaneous nadir overpass approach; Zou and Wang, 2011, 2013). In addition, limb-adjusted brightness temperatures of MSU are also provided in the IMICA calibrated Level-1c files. As such, only adjustments other than sensor inter-calibrations were needed for satellite merging. The IMICA calibrated MSU and AMSU-A radiances and limb adjustments for MSU were described in details in the C-ATBD associated with the MSU and AMSU-A Level-1c radiances dataset (Zou and Wang 2013). This has substantially simplified the processing procedure for developing MSU/AMSU layer temperature TCDR. In summary, the following steps and algorithms are needed to derive the atmospheric layer temperature TCDR:

1. Extracting IMICA-calibrated, limb-adjusted MSU swath brightness temperatures on scan positions for channels 2, 3 and 4 from the IMICA calibrated MSU orbital Level-1c datasets

2. Eextracting IMICA-calibrated (without limb adjustment) AMSU-A swath brightness temperatures on scan positions for channels 5, 7 and 9 from the IMICA calibrated AMSU-A orbital Level-1c datasets

3. Adjusting AMSU-A radiances of off-nadir incident angles to be close to those of the nadir directions

4. Adjusting AMSU-A brightness temperatures due to frequency differences at each scan positions to match MSU observations for their equivalent channels

5. Adjusting the MSU channel 2 and AMSU-A channel 5 brightness temperatures for diurnal drift effect at each scan position

6. Binning limb-, frequency-, and diurnal-adjusted brightness temperatures at scan positions into grid cells of 2.5^{o}x2.5^{o} spatial resolution in monthly interval for each satellite and then averaging the binned data at each grid cell to produce Level-3 layer temperature data for each satellite

7. Removing residual inter-satellite biases including instrument temperature effect using satellite overlap observations of the Level-3 data

8. Bias-removed, multiple satellite Level-3 temperature data are then averaged to generate a 36-year long, merged and homogeneous layer temperature TCDR from 1978 to present. The final product is saved as NetCDF format

3.2 Processing Outline

This section is the general description of the MSU/AMSU layer temperature production system with a set of multiple flowcharts.

3.2.1 Overall Processing Outline

The overall processing outline of MSU/AMSU atmospheric layer temperature TCDR algorithm is summarized in Figure 3-1. Each of the components is described in the following subsections.

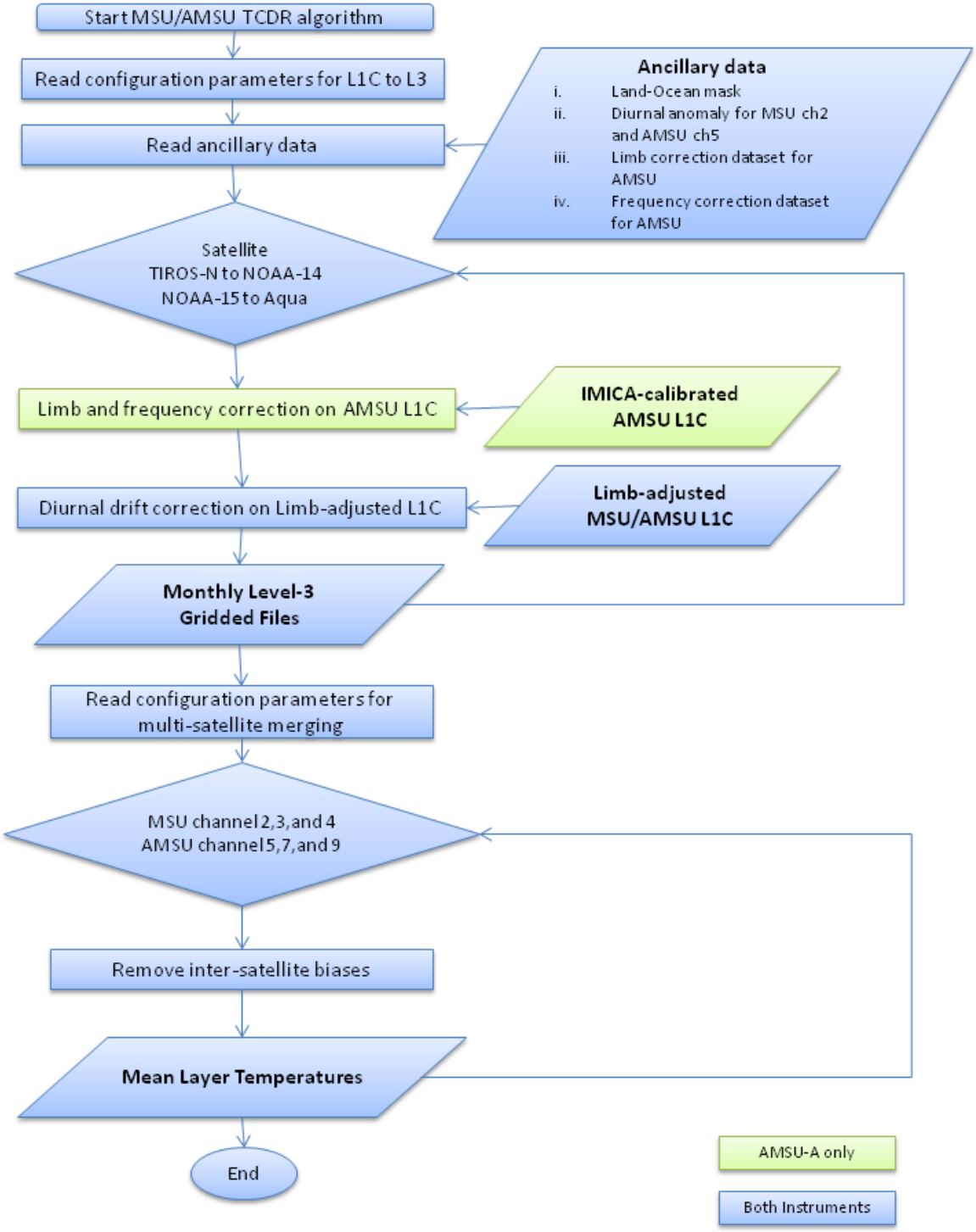

Figure 3-1 High level flowchart of the MSU/AMSU TCDR algorithm illustrating

the main processing section.

3.2.2 System configuration

The system configuration is designed separately for the generation of level 3 layer temperatures of individual satellites and their merged products (Figures 3-2a and 3-2b). Both configurations are common in setting I/O directories and ancillary data directory.

For generation of Level 3 data of individual satellites, the processing uses level-1c files of individual satellites, therefore, satellite names need to be specified and multi thread technique is applied to accelerate the production. Merged product contains TMT, TUT, and TLS derived from MSU channel 2, 3, and 4 and AMSU-A channel 5, 7, and 9, respectively. These are achieved by setting the channel parameter in the system

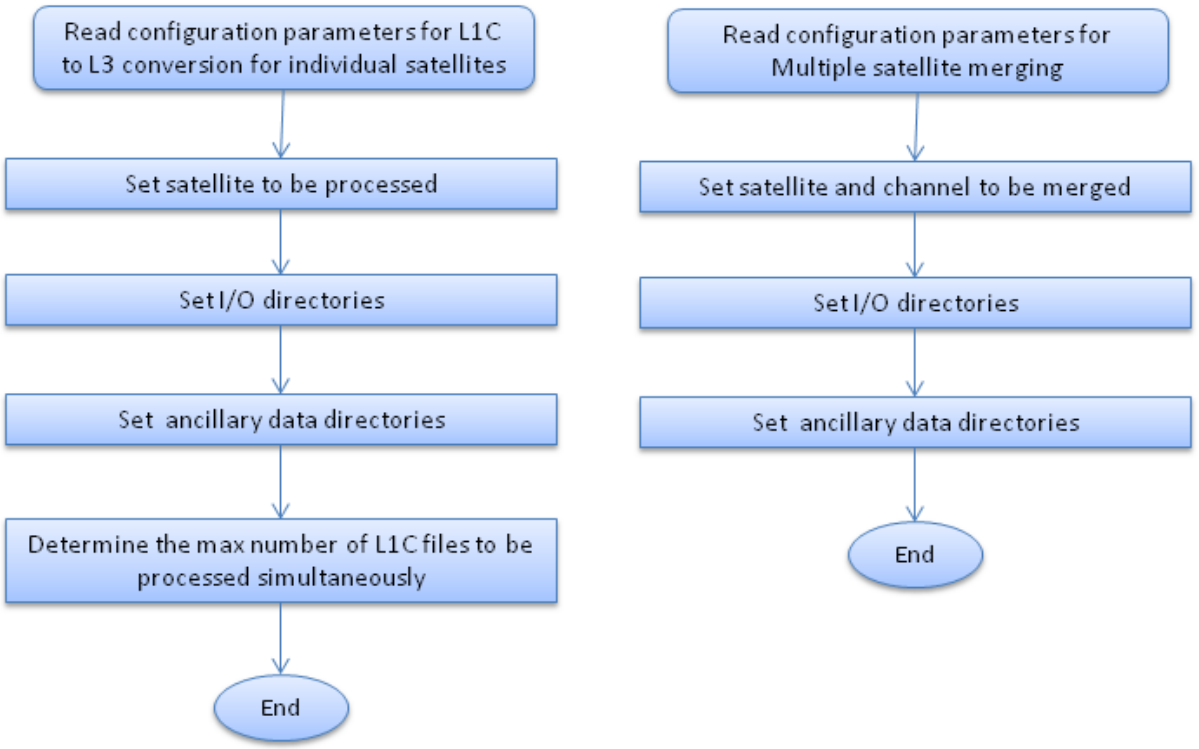

(a) (b)

configuration.

Figure 3-2 Input parameter processing flowcharts for (a) generation of level-3 data of individual satellites and (b) merged layer temperature TCDR for different channels

3.2.3 Preparing Ancillary data

Land-sea fraction data is required for production of both Level-3 data of individual satellites and their merged products (Figure 3-1). For MSU, only diurnal anomaly dataset for channel 2 is required for generating Level-3 data of individual satellites. For AMSU-A, diurnal anomalies for channel 5, limb-adjustment and frequency adjustment datasets for all three channels are required to produce Level-3 data for individual satellites.

3.2.4 Converting Level-1C orbit data to Level-3 gridded data

IMICA calibrated Level-1c data are stored in separated NetCDF files for each orbit. Each file contains necessary information required for TCDR generation such as satellite ID, observation time, geo-location records, warm target temperatures, scene temperatures, quality control flags, etc.

Figure 3-3 illustrates how to use the data and information in Level-1c to generate gridded monthly temperature data (Level-3) for each individual satellite.

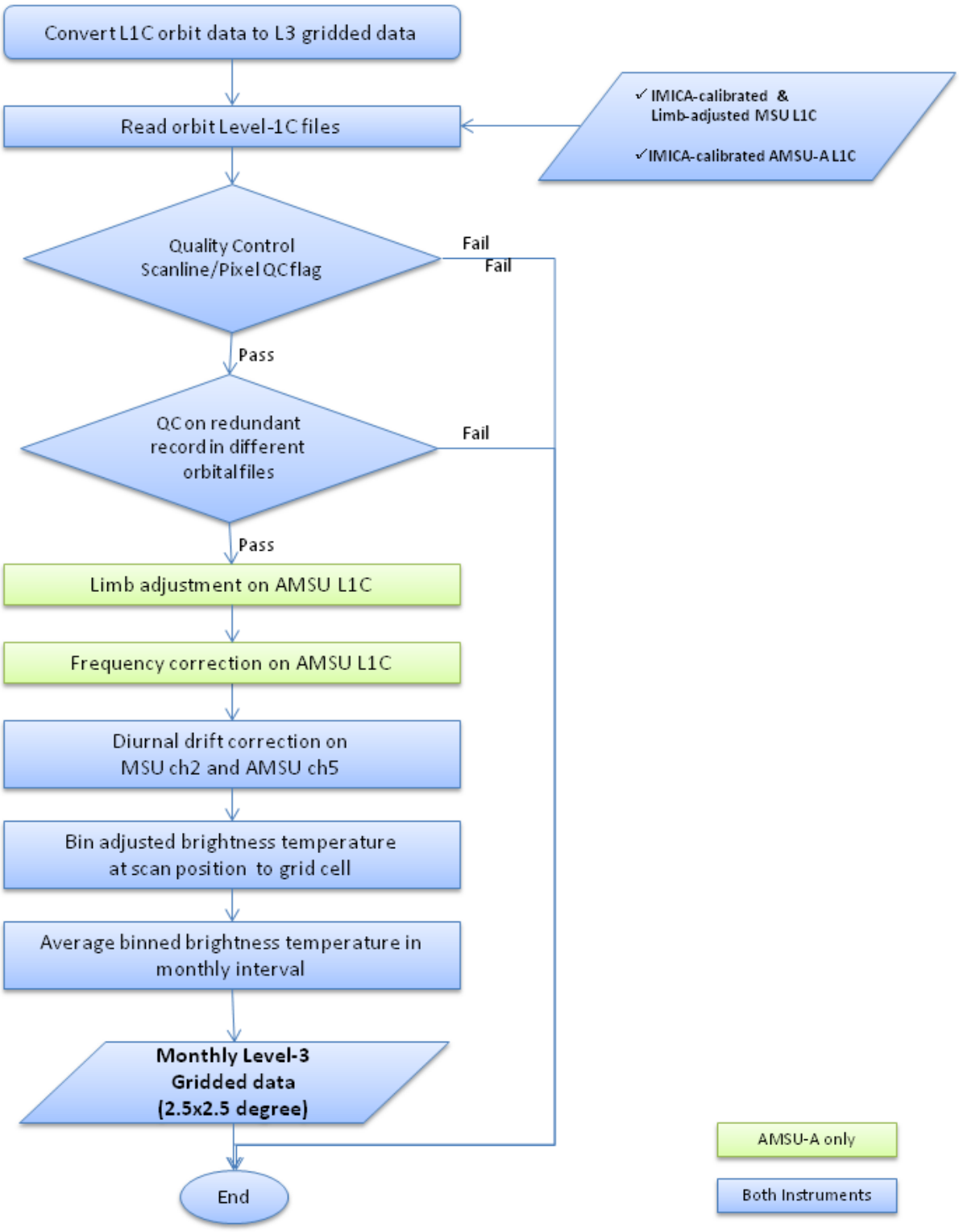

Figure 3-3 Flowchart for processing IMICA calibrated Level-1c brightness temperatures to

generate Level-3 gridded monthly temperature records for individual satellites

3.2.5 Removing inter-satellite biases

Using NOAA-10 as reference, inter-satellite biases between satellite pairs need to be eliminated to produce the merged deep layer temperature records. Figure 3-4 shows the processing steps.

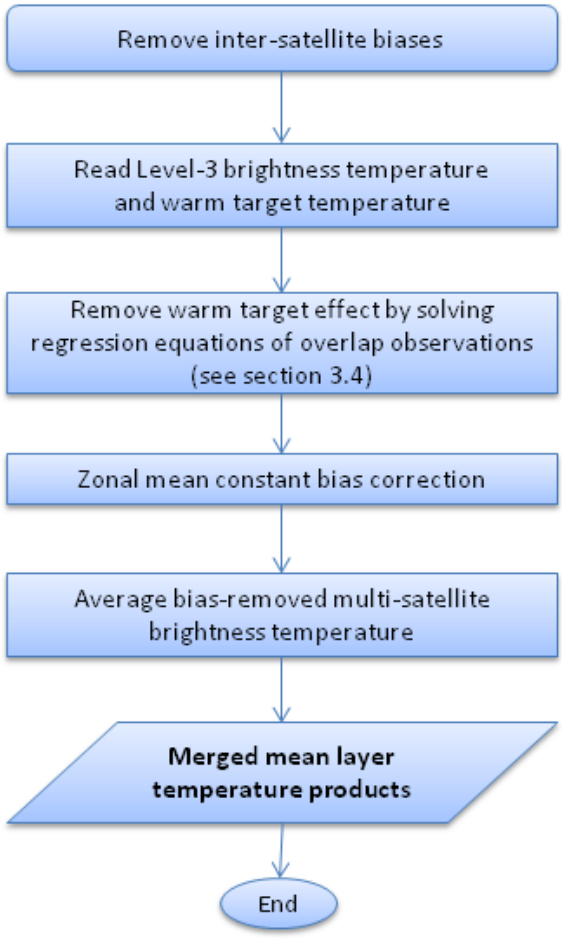

Figure 3-4 Flowchart for processing level-3 gridded monthly temperature records of all satellites to generate merged deep-layer atmospheric temperature products

3.3 Algorithm Input

3.3.1 Primary Sensor Data

The primary sensor data used to derive the atmospheric layer temperature TCDR were the IMICA calibrated, limb-adjusted brightness temperatures saved in the NOAA MSU and AMSU-A radiance FCDR orbital files which were downloaded from the NOAA NCDC CDR website (address: http://www.ncdc.noaa.gov/cdr/operationalcdrs.html). Other primary sensor data also needed were warm target temperatures, geo-location information, and sensor quality flags. These were orbital swath data for each scan positions (Table 3-1). Detailed characteristics of the IMICA calibrated brightness temperatures can be found in the C-ATBD for NOAA MSU/AMSU FCDR (Zou and Wang 2013) available from the NDCD CDR website (http://www.ncdc.noaa.gov/cdr/operationalcdrs.html).

Table 3-1 MSU/AMSU primary sensor data used for developing atmospheric layer temperature TCDR. The dimension 'xsize' is the pixel number per scan-line (11 for MSU, and 30 for AMSU-A) and 'ysize' is the total scan-line number in an orbital file. All these data are available in the NOAA MSU/AMSU radiance FCDR orbital files.

Name	Type	Description	Dimension
Limb-adjusted, IMICA calibrated brightness temperature	Input	Limb-adjusted, IMICA calibrated brightness temperature for MSU channels 2, 3, and 4.	pixel (xsize, ysize)
IMICA calibrated brightness temperature	Input	IMICA calibrated brightness temperature for AMSU-A channels 5, 7, and 9.	pixel (xsize, ysize)
Warm target temperature	Input	Warm target temperatures, average of available good PRT readings	pixel (xsize, ysize)
Latitude	Input	Pixel center latitude	pixel (xsize, ysize)
Longitude	Input	Pixel center longitude	pixel (xsize, ysize)
QC flags	Input	quality control flags from level-1c data	pixel (xsize, ysize)

3.3.2 Ancillary Data

The algorithm requires sets of ancillary data which will be provided in the delivery package.

i. Land-sea mask [A grid cell is considered as ocean (land) if the ocean percentage in the grid cell is greater(smaller) than 50%]

ii. Limb-correction dataset for adjusting AMSU-A observations made at different viewing angles to nadir views (Available in the system package for generation of layer temperature TCDR)

iii. Frequency correction dataset for adjusting AMSU-A observations at different channel frequencies to match MSU temperatures (Available in the system package for generation of layer temperature TCDR)

iv. Diurnal anomaly dataset for diurnal drift correction (Available in the system package for generation of layer temperature TCDR)

3.3.3 Derived Data

The IMICA calibrated MSU and AMSU-A brightness temperatures (radiances) were actually derived data from satellite raw counts data. The derivation procedure was described in details in the C-ATBD for NOAA radiance MSU/AMSU FCDR (Zou and Wang 2013, available from the NCDC CDR website for MSU/AMSU FCDR) and related publications (Zou et al. 2006, 2009; Zou and Wang 2010, 2011). These IMICA calibrated radiances or brightness temperature are treated as primary sensor data as described in Section 3.3.1 since they were directly extracted from the MSU/AMSU radiance FCDR orbital data files.

3.3.4 Forward Models

NOAA/Joint Center for Satellite Data Assimilation (JCSDA) Community Radiative Transfer Model (CRTM) [*Han et al.*, 2006] was extensively used for deriving simulated AMSU-A limb-adjustment and frequency adjustment at each scan positions for corresponding satellite channels. The CRTM model is publicly available through NOAA/JCSDA. The NASA MERRA reanalysis data were used as inputs to the CRTM in all simulations, including surface temperature and atmospheric profiles of temperature, humidity, cloud liquid water, and ozone. The MERRA surface temperature is an hourly data with a grid resolution of 0.5˚ latitude by 0.67˚ longitude. The atmospheric profiles are three hourly data with a grid resolution of 1.25˚ latitude by 1.25˚ longitude. These data were interpolated into those of satellite time and locations for each scan positions for the CRTM to generate simulated correction time series at corresponding swath time and geo-locations for each satellite channels.

3.4 Theoretical Description

This section reviews various bias correction algorithms for developing merged MSU and AMSU-A atmospheric layer temperature TCDR.

3.4.1 Physical and Mathematical Description

Development of atmospheric temperature TCDR involved proper treatment of errors from several different sources. These included, but were not limited to, incident angle effect, diurnal drift errors, warm target effect, short overlaps between certain satellite pairs, central frequency differences of equivalent channels between MSU and AMSU-A, earth-location dependency in inter-satellite biases, orbital-decay and residual biases left from imperfect instrument calibration. Adjustment algorithms for these effects had been developed by NOAA/STAR scientists and other investigators in previous publications for TCDR development. In the following, the physics and algorithms implemented in the NOAA MSU/AMSU-A mean layer temperature TCDR are briefly described.

3.4.1.1 Limb Adjustment

A limb-correction adjusts radiances at off-nadir viewing angles to those close to the nadir direction. This adjustment is necessary for use of the off-nadir footprints in the time series to increase observational samples and reduce noise and sampling-related biases.

Different limb-adjustment approaches were applied for the MSU and AMSU-A instruments, respectively. Limb-adjustment algorithms and coefficients for the MSU observations had been developed by Goldberg et al. (2001) using statistical methods. Zou et al. (2009) examined the impact of the limb-adjustment on the MSU time series and found robust trend results when different limb-corrected footprints were included in the time series. In developing NOAA MSU Level-1c radiance FCDR datasets, limb-adjustment based on Goldberg et al. (2001) approach was applied to the IMICA calibrated radiances for each scan positions. These limb-adjusted radiances were saved in the corresponding MSU Level-1c orbital files which were directly extracted and used in the generation of gridded MSU temperatures. Therefore, limb-adjustment for MSU was not part of the merging algorithms as provided in this software package.

Limb-adjustment applied for the AMSU-A observations was based on Wang and Zou (2014) who developed a limb-adjustment dataset using NOAA CRTM simulations. In this approach, limb-adjustment for each scan positions were obtained as the CRTM simulated differences, with NASA MERRA reanalysis as inputs to the simulation, between those with off-nadir and zero scan angles. The approach was different from the Goldberg et al. (2001)'s which adjusts a target channel using adjacent channels. The performances of the two methods are comparable in the absence of malfunctioning channels. However, multiple AMSU-A channels failed during satellite operations in which the Goldberg et al. (2001) algorithm was inapplicable. The limb-adjustment based on CRTM simulations does not depend on neighbor channels and thus can provide adequate adjustments in all situations. This maximizes utilizations of AMSU-A observations.

The original limb-adjustment dataset in Wang and Zou (2014) was provided for each scan positions for all satellites during their entire operational periods. To simplify the process, a

yearly-mean monthly limb-correction climatology was obtained by converting the original limb-corrections at scan potions to grid cells with a spatial resolution of 2.5^{o} longitudes by 2.5^{o} latitudes for all individual satellites. Our sensitivity studies indicated that this conversion produced a limb-adjustment with accuracy similar to the Goldberg et al. (2001) approach (Figure 3-5) and thus did not affect the merging accuracy. As a result, in this CDR, the limb-adjustment for AMSU-A instrument used a dataset with 144 (longitude) x 72 (latitude) x 12 (month) dimensions for each satellite, and this dataset is included in the software package.

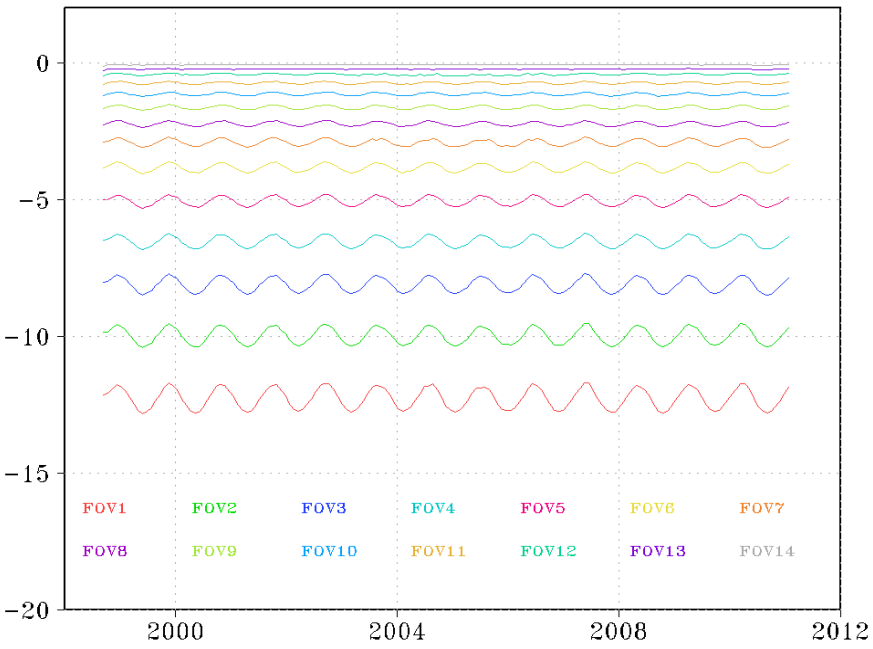

(a)

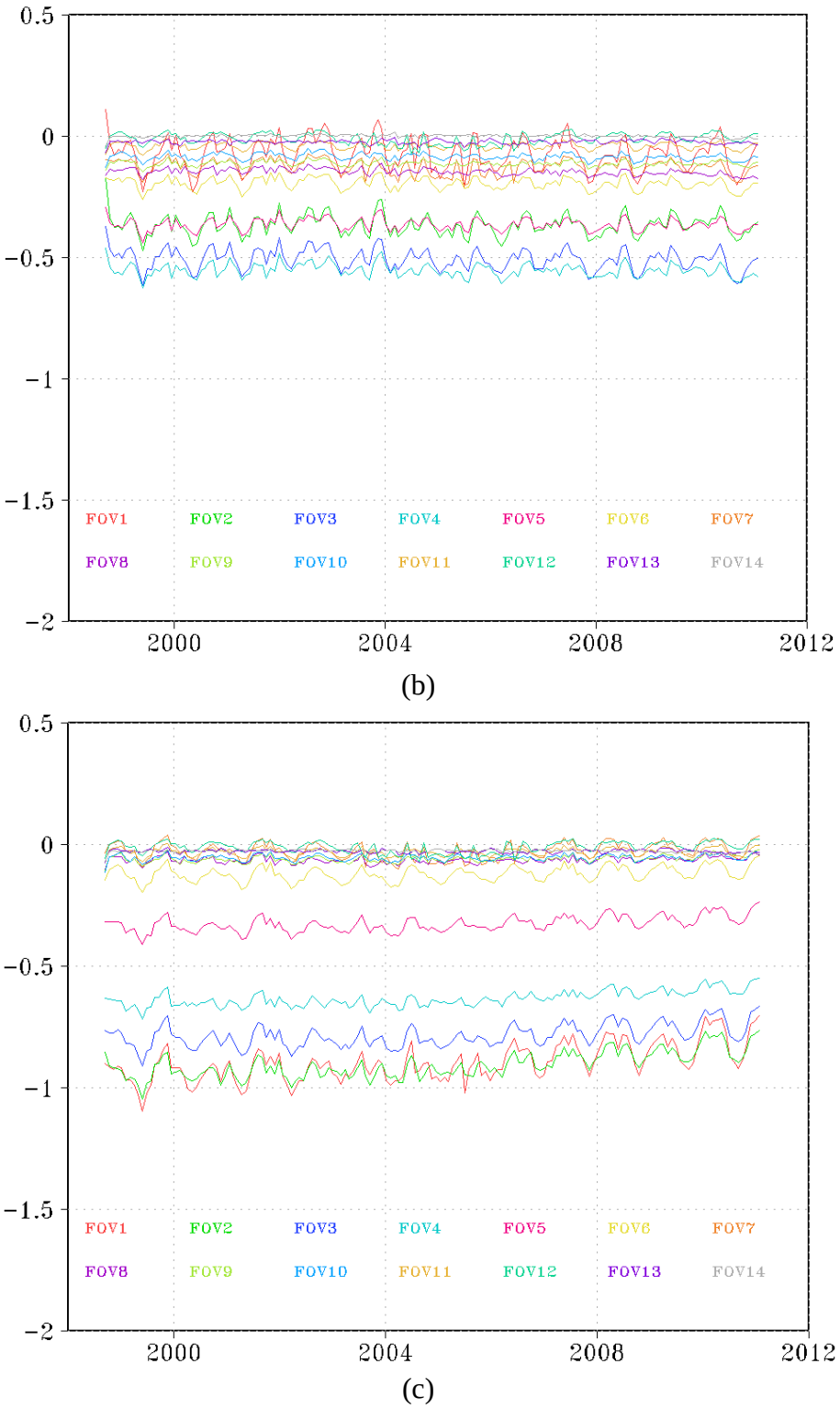

Figure 3-5 Time series of the off nadir biases for NOAA-15 channel 5 for scan

positions 1-14 for (a) without limb-adjustment; (b) with limb-adjustment using the yearly mean monthly climatology with gird resolution of 2.5° latitudes by 2.5° longitudes; (c) with Goldberg et al. (2001) limb-adjustment approach. The two approaches perform similarly for near nadir views while the climatology approach performs better for the near limb views.

3.4.1.2 Diurnal Drift Correction

The diurnal drift effect was caused by satellite orbital drift which resulted in changes in local observational time that, if not corrected, may introduce false climate trend by introducing diurnal trend into it. Orbital differences between morning and afternoon satellites also caused differences in observational time. Averages of satellite ascending and descending orbits cancel out the diurnal mode in the drift effects, but the asymmetric semi-diurnal mode between day and night in the diurnal changes cannot be canceled out in the averaging process. Its effect is particularly large for land areas of the mid-tropospheric channel (MSU channel 2 and AMSU-A channel 5) where diurnal amplitude is large.

Techniques for removing the diurnal-drift effect in this CDR development were to adjust the scene brightness temperatures at different observational time from all different satellites to a common 12-noon local time before binning them into grid cells. This process is expressed by

$$T_{ba}(\mathbf{X}, t_{12-noon}) = T_b(\mathbf{X}, t) - \Delta T \qquad (1)$$

where $T_b(\mathbf{X}, t)$ represents the IMICA-intercalibrated and limb-adjusted Level-1c scene brightness temperature at time t and geographic location $\mathbf{X}$, $T_{ba}(\mathbf{X}, t_{12-noon})$ the adjusted brightness temperature at the 12-noon local time, and $\Delta T = T_{bs}(\mathbf{X}, t) - T_{bs}(\mathbf{X}, t_{12-noon})$ an estimated diurnal anomaly used for the adjustment. The diurnal anomaly is a function of time and geo-location. In this CDR, the Remote Sensing Systems (RSS) diurnal anomalies were adopted in the correction. The RSS diurnal anomaly was a monthly mean hourly dataset developed from climate model simulations (Mears et al. 2003). The dataset may contain potential errors due to climate modeling uncertainties. To minimize these errors, a diurnal scaling factor was introduced by matching observations. The scaling factor was found to be 0.875 for MSU and 0.917 for AMSU-A by minimizing inter-satellite differences over land, which resulted in best fitting of satellite overlaps over land and consistent temperature trends between land and oceans (Zou and Wang 2010).

The above process effectively eliminated diurnal drift effects for TMT. TUT and TLS did not include diurnal drift adjustment since its effect was negligible for these channels (Zou et al. 2009; Zou and Wang 2010).

3.4.1.3 Frequency adjustment for AMSU-A radiances

Due to differences of channel frequencies, weighting functions of the MSU and AMSU-A instruments are slightly different for their equivalent channels (Figure 2-1). These differences in weighting functions translate to scene temperature differences between the two instruments due to non-zero atmospheric lapse rate. These scene temperature differences also change with scan positions for each channel due to atmospheric lapse rate differences over height, geo-location, and time. These temperature differences must be removed before the two instrument observations are merged together for CDR generation. In this CDR, the frequency adjustment was obtained as the CRTM simulated differences between those with AMSU-A and MSU channel frequencies for each scan position, each channel, and each AMSU-A satellite, using NASA MERRA reanalysis as inputs in the simulations. Mathematically, the process is represented as:

$$T_{eq}(sat, ch, p) = T_o(sat, ch, p) - \Delta T \qquad (2)$$

where $T_o(sat, ch, p)$ represents the original IMICA-intercalibrated AMSU-A swath scene brightness temperature at an individual scan position for individual channels (e.g. channels 5, 7, and 9) and satellites, while $T_{eq}(sat, ch, p)$ is the equivalent brightness temperature corresponding to MSU channels (channels 2, 3, and 4, respectively) after adjustment by ΔT, which is the simulated brightness temperature differences due to the central frequency differences between the two instruments.

In actual applications, the simulated frequency adjustment, ΔT, at each scan positions for each channel were converted to a yearly mean monthly climatology with spatial resolution of 2.5^o longitudes by 2.5^o latitudes for all individual satellites. This frequency adjustment dataset is included in the software package.

3.4.1.4 Instrument temperature variability in radiances

The warm target was an onboard blackbody used to calibrate the MSU and AMSU-A raw observations for obtaining level-1c radiances. The warm target temperature was measured by the Platinum Resistance Thermometer (PRT) embedded on the blackbody. However, this temperature incurred a large variability and trend due to solar heating on the instrument, which originated from seasonal changes in solar angles relative to the satellite orbit normal over a year and its yearly differences due to orbital-drift (Zou and Wang 2011). This variability and trend was mostly removed by IMICA level-1c calibration (Zou et al. 2009, Zou and Wang 2010, 2011), however, small residual variability and biases may still exist due to imperfect calibration. These small residual biases need to be further removed before merging the satellite data for TCDR generation. Christy et al. (2000) developed an empirical algorithm to remove radiance variability due to this warm target effect. This approach finds a best fit empirical relationship between the correction term of the Level-3 gridded brightness temperatures and warm target temperatures and

then removes the best fit from the unadjusted time series. It was shown that using this empirical approach on top of the IMICA level-1c calibration yielded MSU/AMSU trends that meet their stability requirement (Zou and Wang 2010).

Using T_{ba} and T_{bu} to respectively represent adjusted and unadjusted brightness temperatures, this empirical approach can be mathematically expressed as

$$T_{ba} = T_{bu} + b_j - b_k + a_j T_w^{'}(j) - a_k T_w^{'}(k) \qquad (3)$$

where $T_w^{'}$ denotes the global ocean mean warm target temperature anomaly, and the subscripts j and k represent satellite indexes in a satellite pair. The satellites j and k went through all NOAA polar orbiting satellites from TRIOS-N to NOAA-18, as well as MetOp-A and AQUA. This forms a set of multiple satellite regression equations. Assuming NOAA-10 as a reference satellite so that b(NOAA-10)=0, then the constant ($b_j - b_k$) between satellites j and k and the target factors a_j and a_k for all other satellites were solved simultaneously from these multiple satellite regression equations using ocean-mean overlapping observations.

3.4.1.5 Correction of the Earth-Location Dependent Biases

Although IMICA calibration minimized inter-satellite biases in the Level-1c radiances, zonal dependent inter-satellite biases may still exist for certain channels on certain satellites in the Level-3 gridded time series (Zou et al. 2009). This occurred because the nonlinearity of the Level-1c calibration equation was assumed to be of quadratic type. It is possible that higher order nonlinearities exist for certain channels and these unresolved nonlinearities may cause inter-satellite biases to depend on latitudes (Zou et al. 2009). To remove these biases, a zonal dependent constant bias correction was always applied as a final step before merging the satellite data. This correction ensures inter-satellite biases at all latitudes to be minimized so that more reliable regional trends may be obtained from the merged time series.

3.4.2 Data Merging Strategy

After applying the set of adjustments mentioned in the previous sections, the mean of the inter-satellite biases was numerically close to zero. The standard deviation of the inter-satellite biases was also significantly reduced compared with unadjusted data. As a result, the MSU and AMSU-A layer temperature data from different spacecrafts can be treated as a homogenous CDR and then these observations were simply averaged on each grid cells to obtain a merged layer temperature TCDR.

3.4.3 Numerical Strategy

Most of the bias adjustment procedures are straightforward in numerical calculations once the IMICA level-1c radiances are extracted from MSU and AMSU-A

radiance FCDR data files. However, removing warm target temperature effect requires solving a set of multiple satellite regression equations. This requires a computer system to contain an internal library which has a software program to be called directly for solving multiple linear equations.

3.4.4 Calculations

The calculation steps for generating the MSU/AMSU atmospheric layer temperature records are as follows:

1) Read ancillary datasets including land-sea fraction and diurnal anomaly dataset

2) Processing each MSU level-1c orbital files

   - Read in information including quality control flags, geo-location, observational time, warm target temperature, scene temperature, etc.
   - Continue processing qualified data records
   - Skip redundant temperature records
   - Diurnal drift correction for MSU channel 2
   - Bin the warm target temperatures and scene brightness temperatures at scan positions into grid cells in a monthly interval

3) Processing each AMSU-A level-1c orbital file

   - Read in information including quality control flags, geo-location, observational time, warm target temperature, scene temperature, etc.
   - Continue processing qualified data records
   - Skip redundant temperature records
   - Limb correction for AMSU-A channel 5, 7, and 9
   - Frequency adjustment for AMSU-A channels 5, 7, and 9
   - Diurnal drift correction for AMSU-A channel 5
   - Bin the warm target temperatures and scene brightness temperatures at scan positions into corresponding time slots and grid cells

4) Repeat steps 2) and 3) until all level-1c files are processed and level-3 NetCDF files are generated for all satellites

5) Processing equivalent channels for the MSU and AMSU-A instruments

   - Read in gridded level-3 brightness temperatures of an equivalent channel for both MSU and AMSU-A instruments and their corresponding gridded warm target temperatures for all satellites

   - Solve for regression coefficients (target factors) of the multi-satellite regression equations for removing warm target effect. NOAA-10 was defined as a reference

   - Perform zonal mean constant bias correction

   - Generate merged layer temperature records

6) Stop after all channels are processed

3.4.5 Look-Up Table Description

The RSS diurnal anomaly dataset is actually a look-up table. It provides diurnal anomaly values (ΔT, Equation 1) relative to a daily average. It is a yearly mean hourly data available for each day for the 12 months in a year. For a satellite observation falling within a specific day and month between two evenly hours, diurnal adjustment converts the observations to the 12-noon local time based on the look-up table (Equation 1).

In addition to diurnal anomaly dataset for channel 5, two more look-up tables are required for the AMSU-A processing. These are limb adjustment and frequency adjustment datasets generated from CRTM simulations. At each pixel of AMSU-A observations, there are corresponding limb and frequency corrections to adjust the off-nadir radiances for AMSU-A channels 5, 7, and 9 to near-nadir views of equivalent MSU observations of channel 2, 3, and 4, respectively.

3.4.6 Parameterization

N/A

3.4.7 Algorithm Output

More than Thirty-six-year of MSU/AMSU combined monthly atmospheric layer temperatures, including TMT, TUT, and TLS, are the output products. The datasets have global coverage with 2.5^0x2.5^0 grid resolution covering time period from October 1978 to present. All products are in NetCDF format which meet the requirements of *NetCDF Metadata Guidelines for IOC Climate Data Records*.

4. Test Datasets and Outputs

4.1 Test Input Datasets

The MSU/AMSU atmospheric layer temperature TCDR has such a high accuracy and precision that no other datasets are good enough to validate it. Reproducibility and accuracy of the datasets can only be demonstrated by examining the accuracy and precision of the merging algorithm. Algorithm evaluation was conducted in many different ways for the MSU/AMSU layer temperature TCDR (Zou et al. 2009, Zou and Wang 2010) and they are summarized below.

4.2 Test Output Analysis

4.2.1 Reproducibility and Accuracy

The MSU/AMSU atmospheric layer temperature TCDR was derived from merging MSU and AMSU-A observations onboard multiple satellites and its primary purpose was to detect climate trends. As such, accuracy and precision of the merging algorithm is critical to determine the dataset accuracy in trend detection. A quantitative approach for assessing the accuracy and precision of the merging algorithm is to examine inter-satellite biases. Ideally, inter-satellite biases must be zero throughout satellite overlaps; otherwise, bias drifts between satellite pairs may cause ambiguity in the resulting trends.

Figure 4-1 demonstrates the performance of the algorithm by showing global ocean (Figure 4-1a) and land (Figure 4-1b) mean difference time series between all satellite pairs for their overlapping observations for the IMICA calibrated data, which are the inputs to the algorithm, compared to those after all bias corrections were implemented. As seen, small inter-satellite biases on the order of 0.2 K existed for the IMICA calibrated brightness temperatures for satellite pairs other than NOAA-14 and NOAA-15 for which inter-satellite biases reached 2K due largely to the frequency differences between MSU and AMSU-A observations. After applying bias corrections including diurnal drift correction, frequency adjustment, removal of warm target effect, and constant inter-satellite bias correction, inter-satellite biases became zero over all overlapping observations between satellite pairs. Furthermore, the standard deviation of the inter-satellite difference time series was also minimized. Table 4-1 compared the mean standard deviations for all satellite pairs before and after applying bias correction algorithms to the IMICA calibrated brightness temperatures. These zero inter-satellite biases and minimized standard deviation of the global mean inter-satellite differences are the two primary quantities ensuring accuracy and precision of the merged layer temperature TCDR.

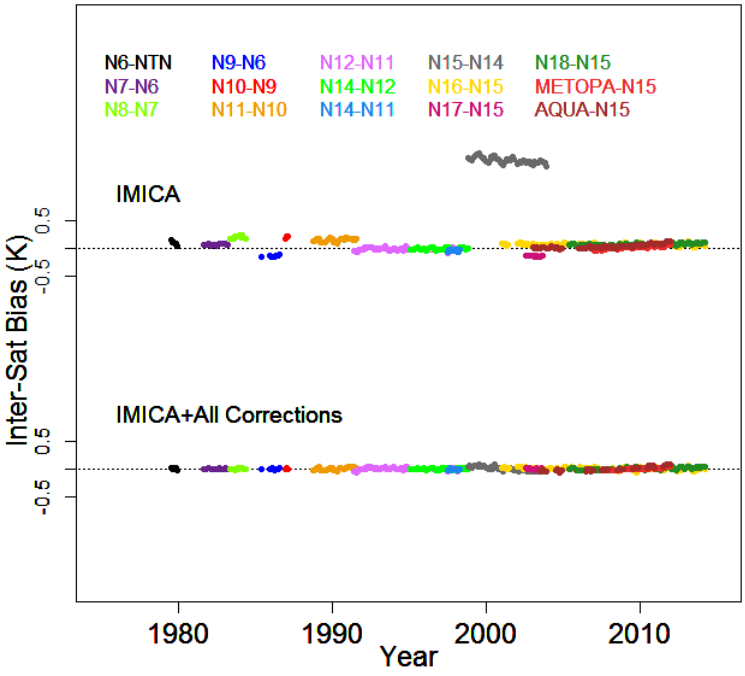

(a)

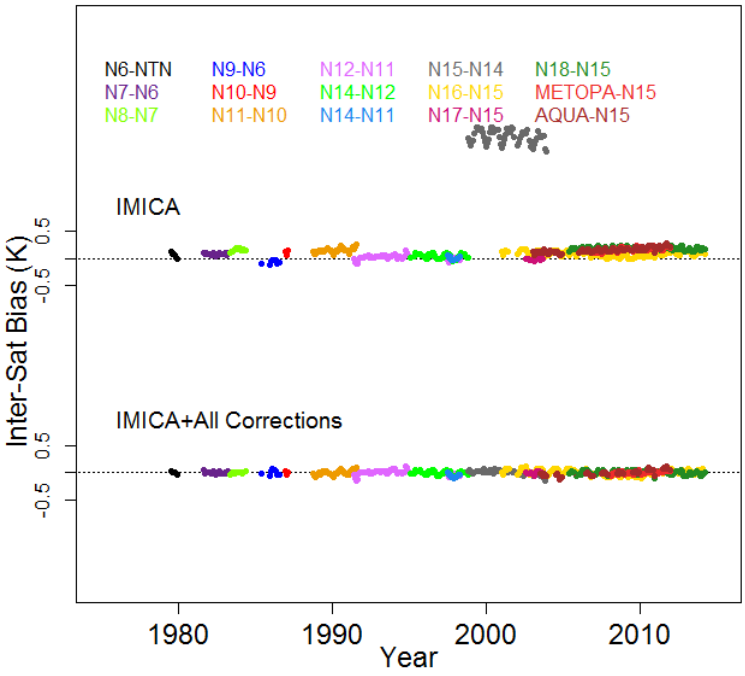

(b)

Figure 4-1 Global ocean-mean (a) and land-mean (b) inter-satellite brightness temperature difference time series for MSU channel 2 onboard TIROS-N through NOAA-14 and AMSU-A channel 5 onboard NOAA-15 through MetOp-A

and NASA Aqua for the IMICA inter-calibrated radiances (top lines) and after applying all bias corrections to the IMICA calibrated radiances (bottom lines).

Table 4-1 Mean standard derivation (K) of global mean inter-satellite difference time series for overlapping observations between all satellite pairs for both the IMICA calibrated (input) and after applying all bias correction algorithms.

	IMICA Calibrated Radiances		IMICA+ all bias correction algorithms	
Products	*Ocean mean*	*Land mean*	*Ocean mean*	*Land mean*
TMT	0.024	0.054	0.019	0.048
TUT	0.037	0.049	0.030	0.041
TLS	0.040	0.042	0.033	0.040

Two additional methods were also used to ensure reproducibility of the trends of the products. The first one was to compute global means of level-3 gridded products for each satellite and then applying bias correction algorithm to these global means. The merging of the global mean data from different satellites may yield more reliable trend since random errors from grid cells were averaging out in the global mean process so the bias structures were believed to be simpler in global means (Zou et al. 2009). The trend from the global mean merging was then compared to the global mean trends calculated from the gridded layer temperature TCDR and Table 4-2 showed the results. It is seen that the two methods yielded nearly identical trends from 1978-2006, indicating robustness and reproducibility of the gridded products in trend detection.

Table 4-2 Global mean temperature trends (K/Decade) for 1978-present derived from global mean merging and averages of spatial trends of the gridded products.

Product	Global mean trend from global mean merging	Global mean trend from averaging spatial trend of TCDR
TMT	0.095	0.105
TUT	0.030	0.040

TLS	-0.304	-0.310

The second approach was to examine trend differences between land and oceans. It is expected that trends over the global land and ocean are consistent with each other since the atmosphere is well-mixed for the long-term climate process (Zou and Wang 2010). The diurnal drift correction has significant impact on trends over the land. After diurnal correction, trends over the global land and oceans are identical for TMT (Table 4-3). This indicated that diurnal drift correction has met the accuracy requirement for the merging.

Table 4-3 Mean layer temperature trends (K/Decade) during 1978-present for global ocean mean and global land mean

Product	Trend of global ocean mean	Trend of global land mean
TMT	0.105	0.105
TUT	0.035	0.044
TLS	-0.308	-0.313

4.2.2 Error Budget

Total uncertainty of the MSU/AMSU layer temperature products are between 0.5 to 1 K. This is the uncertainty when merged temperatures (not anomalies) are compared to observations from other instruments such as radiosondes or Global Positioning System Radio Occultation (GPSRO). This uncertainty is the absolute bias of the MSU/AMSU layer temperature products which arise from many different sources of errors such as inaccurate instrument calibration, side-lobe effect, and antenna pattern correction, etc. Although relatively large, this uncertainty is believed not to significantly change with time after different satellite instruments were inter-calibrated against a reference satellite. Since absolute values of the observations are unknown and there are no SI-traceable standards to compare with, this absolute bias cannot be removed. In layer temperature time series, this uncertainty is treated as a constant which does not affect trends. The changing with time of this uncertainty is measured by the stability of the temperature products, which was determined by sensitivity experiments. Zou et al. (2009) investigated changes of the mean trends versus different total footprint numbers per scan line used in generating the layer temperature TCDR. It was found that maximum trend differences between different footprint numbers are within 0.02 K/Decade for all channels in different experiments, showing robust trend values when more independent pixel observations were included. This experiment gave a MSU/AMSU stability about 0.02 K/Decade.

Table 4-4 summarized error budget for the layer temperature TCDR.

Table 4-4 Error budget

Error Type	Error Range	Comments
Calibration Uncertainty	0.5 - 1 K	This is total absolute uncertainty in instrument calibration, which is treated as a constant
Stability of TCDR	0.02 K/Decade	This stability is a measurement of bias drift relative to a benchmark climate observation that is assumed with no bias drift. This value was obtained by sensitivity studies
Global mean inter-satellite biases	0.00 K	After bias corrections, mean biases of global mean overlap observations reach zero
Standard deviation of global mean inter-satellite differences	0.02-0.03 K	This is for TMT. Stratospheric temperature products may have a higher value up to 0.05 K

5. Practical Considerations

5.1 Numerical Computation Considerations

1. To speed up the generation of level-3 data (from swath scene brightness temperature to gridded temperature), multithread technique is employed in TCDR software code. This technique allows the TCDR software to run faster on a computer system that has multiple CPUs, CPU with multiple cores, or across a cluster of machines. Multiple MSU level-1c files can be processed simultaneously to produce level-3 files with this approach.

2. Unqualified level-3 data: The monthly level-3 data of individual satellites may incur relatively larger errors in certain months. This may be caused by insufficient swath scene temperatures and invalid level-1c scan lines, etc, for the month. It may lead to outliers in the merged time series. To ensure high quality of dataset, all monthly level-3 files generated from the level-1c were sifted manually month by month before applying bias correction and merging algorithms.

5.2 Programming and Procedural Considerations

MSU/AMSU TCDR software package does not implement any numerical model.

5.3 Quality Assessment and Diagnostics

The quality of the final products was evaluated in the following ways:

1. Inter-satellite biases for each satellite pair during their overlapping period is evaluated as an indicator of the product quality and accuracy of merging algorithm. Mean inter-satellite biases were shown to be zero and standard deviations were minimized compared to those without bias corrections. These indicated high quality and accuracy of the merged products.

2. As discussed in the algorithm accuracy section, trend consistencies between land and ocean and between different merging methods served as another indicator of product quality.

3. Monthly images of the layer temperatures for the entire observational period from 1978-present were put on the project website for frequent check of possible data quality issues

   (see http://www.star.nesdis.noaa.gov/smcd/emb/mscat/imageBrowser.php). If outliers were found for a particular month, input data will be reexamined to find the root causes and then more rigorous quality controls on the input data will be implemented until the problem is resolved. Animation of monthly images show

continuous changes of the climate event both locally and globally, indicting high quality of products.

5.4 Exception Handling

Exceptions considered in the MSU/AMSU processing codes include:

1. Class Not Found Exception will be reported and the system stops running when the code tries to load in a class but no definition for the class could be located due to misplacement of external libraries

2. Out of Memory Exception will be identified when the system cannot allocate a block a memory. If this exception occurs, the system will report the exception and exit running

3. File Not Found Exception will be reported and the system exits running when an ancillary file does not exist or inaccessible

4. EOF Exception will be reported when an end of file has been reached unexpectedly during file reading operations

5. IO Exception will be reported and the system stops running when a failed I/O operation, other than exceptions 3 and 4, occurs.

5.5 Algorithm Validation

As described in sections 4.1, 4.2 and 5.3.

5.6 Processing Environment and Resources

Table 5-1 lists the environment and resource requirements for the MSU/AMSU TCDR processing codes.

Table 5-1 Processing environment and resource requirements.

Computer Hardware	Minimum Configuration: Processor: 2.0GHz Memory: 100 MB Disk Space 100 GB A system with multiple CPUs is preferred
Operating System	Linux or Windows
Programming Languages	JAVA Bash script
Compilers	Sun JAVA Compiler

External Library	NetCDF-JAVA 4.1 Jscience4.3
Storage Requirement	100GB
Execution Time Requirement	Single CPU ~72 hours for 15 satellites Varied when using parallel computing

6. Assumptions and Limitations

6.1 Algorithm Performance

NOAA-10 was assumed as a reference satellite during the merging process, meaning all satellites were adjusted to observations from NOAA-10. However, biases relative to an unknown absolute truth may exist in NOAA-10 MSU observation. The actual value of this bias cannot be determined since no SI-traceable standard exist at the time of this writing for the MSU/AMSU observations.

6.2 Sensor Performance

The stability of the MSU/AMSU temperature trends depends on performance of the sensor channel frequencies, which were assumed to be stable for all satellite channels. Possible MSU and AMSU-A frequency shift is a current research topic. If it is confirmed in the future that MSU and AMSU-A channel frequency incurred shift during satellite operations, additional adjustment may need to be implemented for algorithm consistency and product accuracy. Methods for frequency adjustments had been developed for merging MSU and AMSU-A channels at NOAA/STAR. These methods can be adopted for merging MSU and AMSU-A channels with frequency shift.

7. Future Enhancements

Current CDR products are generated based on the understanding of currently available radiances data. Since AMSU-A is under operational status, continuous observations are accumulated which will modify our insight of the data and implies the possibility of the adjustment on bias correction scheme, even on radiances calibration algorithm, in the future.

During the development of current algorithm, the radiances from AMSU-A onboard NOAA-19 have not been considered due to the limited period of observation. The IMICA-calibration will be applied for AMSU-A on NOAA-19, and eventual being included in CDR product, when resource is permissible. Involving of new instrument will definitely affect the strategy of bias correction and inter-satellite merging. The stability and the accuracy of the products are expected to be improved because introduction of an independent historical observation will serve to further reduce the uncertainty.

Diurnal drift adjustment generally contains larger uncertainty and it affects TMT trends over the land areas. Research is being conducted to find more accurate diurnal anomaly datasets that can improve the TMT products over the entire land area and the entire observational period. If such datasets were found, an update of the TMT product will be provided with improved diurnal drift corrections.

8. References

Christy,J.R., R.W. Spencer, W.D. Braswell (2000). MSU tropospheric temperatures: Dataset construction and radiosonde comparisons. *J. Atmos. Oceanic. Technol.* 17:1153–1170

Goldberg, M.D., D.S. Crosby, L. Zhou (2001). The limb adjustment of AMSU-A observations: methodology and validation. *J. App. Meteor.* 40:70–83.

Kidwell, K.B., edited, (1998). NOAA Polar Orbiter Data User's Guide, available at **http://www.ncdc.noaa.gov/oa/pod-guide/ncdc/docs/podug/index.htm**

Mears, C.A., M.C. Schabel, F.J. Wentz (2003). A reanalysis of the MSU channel 2 tropospheric temperature record. *J. Climate* 16:3650–3664

Robel, J., et al. edited, (2009). NOAA KLM user's guide, available at http://www.ncdc.noaa.gov/oa/pod-guide/ncdc/docs/klm/index.htm

Wang, Wenhui, Cheng-Zhi Zou, 2014: AMSU-A-Only Atmospheric Temperature Data Records from the Lower Troposphere to the Top of the Stratosphere. *J. Atmos. Oceanic Technol.*, 31, 808-825, DOI: 10.1175/JTECH-D-13-00134.1

Zou, C.-Z., *et al.* (2006). Recalibration of microwave sounding unit for climate studies using simultaneous nadir overpasses. *J. Geophys. Res.*, 111(D19), D19114

Zou, C.-Z., *et al.* (2009). Error structure and atmospheric temperature trends in observations from the Microwave Sounding Unit. *Journal of Climate*, 22(7), 1661-1681

Zou, C.-Z., and W. Wang (2010). Stability of the MSU-derived atmospheric temperature trend. *Journal of Atmospheric and Oceanic Technology*, 27(11), 1960-1971

Zou, C.-Z., and W. Wang (2011). Intersatellite calibration of AMSU-A observations for weather and climate applications. *J. Geophys. Res.,* 116(D23), D23113

Zou, C.-Z. and W. Wang (2013). MSU/AMSU Radiance Fundamental Climate Data Record Calibrated Using Simultaneous Nadir Overpasses Climate Algorithm Theoretical Basis Document (C-ATBD), NOAA/NESDIS

Appendix A. Acronyms and Abbreviations

Acronym or Abbreviation	Meaning
AMSU	Advanced Microwave Sounding Unit
CATBD	Climate Algorithm Theoretical Basis Document
CDR	Climate Data Record
CDRP	Climate Date Record Program
CRTM	Community Radiative Transfer Model
EUMETSAT	European Organisation for the Exploitation of Meteorological Satellites
FCDR	Fundamental Climate Data Record
FOV	Field of View
GPSRO	Global Positioning System Radio Occultation
IFOV	Instantaneous Field of View
IMICA	Integrated Microwave Inter-Calibration Approach
MERRA	NASA's Modern-Era Retrospective Analysis for Research and Applications
MetOp-A	The European Meteorological Operational satellite program-A
MSU	Microwave Sounding Unit
NCDC	National Climatic Data Center
NESDIS	National Environmental Satellite, Data, and Information Services
NetCDF	Network Common Data Form
NASA	National Aeronautics and Space Administration
NOAA	National Oceanic and Atmospheric Administration
PRT	Platinum Resistance Thermometer
RSS	Remote Sensing Systems
SNO	Simultaneous Nadir Overpass
STAR	Center for Satellite Applications and Research
TCDR	Thematic Climate Data Record
TLS	Temperature of lower-stratosphere
TMT	Temperature of mid-troposphere
TUT	Temperature of upper-troposphere